A law controlling polymer recrystallization showing up in experiments on s-polypropylene

Barbara Heck[1], Silvia Siegenführ[1], Gert Strobl[1] and Ralf Thomann[2]

[1]Physikalisches Institut

[2]Institut für Makromolekulare Chemie

Albert-Ludwigs-Universität Freiburg

79104 Freiburg

Germany

Abstract

When polymers are crystallized at large supercoolings a subsequent heating is accompanied by recrystallization processes, which proceed to a fixed final melting point. We studied these processes with small angle X-ray scattering and DSC measurements for three s-polypropylenes with different stereoregularity and co-unit content. As is known from previous experiments, crystal thicknesses d_c depend on the crystallization temperature T_c only, being not affected by stereo defects or co-units. The new experiments, all carried out for low crystallization temperatures, again confirm this property; in plots of d_c^{-1} versus T_c all points are located on a unique straight crystallization line. A similarly simple law controls the crystal thickness during the continuous structure reorganization on heating. Over an extended temperature range d_c^{-1} changes linearly with temperature, guided by a unique, i.e. sample-invariant, 'recrystallization line'. Crystallization and recrystallization line extrapolate for $d_c^{-1} \to 0$ to the same limiting temperature, T_c^{∞}, and differ only in slope. The findings indicate that both the initial crystallization at T_c and the process of recrystallization use a pathway via a transient mesomorphic

phase. The DSC thermograms of the samples show a multiple peak structure which varies with the heating rate. The SAXS results enable the peaks to be assigned to different melting processes.

1 Introduction

Several years ago we carried out a comprehensive small-angle X-ray scattering (SAXS) investigation on s-polypropylene and related octene copolymers with the objective to determine the relationships between the crystallization temperature (T_c), the crystal thickness (d_c) and the melting temperature (T_f) [1]. The findings in this study included some unexpected features. Conventional wisdom assumed that crystal thicknesses are controlled by the supercooling below the respective equilibrium melting point T_f^∞, but this was not observed. It was found that, for all samples in common, thicknesses are inversely proportional to the distance to a certain temperature T_c^∞ which is located above all the equilibrium melting points. On the other hand, the melting points varied with the crystal thickness as described by the Gibbs-Thomson equation, and they decrease when the co-unit content is increased. Fig. 1 reproduces once again these results:

- When d_c^{-1} is plotted as a function of T_c all points are located on a unique 'crystallization line'. Extrapolation of the line to $d_\mathrm{c}^{-1} = 0$ leads to T_c^∞=195°C .
- The Gibbs-Thomson melting lines T_f versus d_c^{-1} of the different samples have a common slope and shift their position downward when the co-unit content increases.
- Crystallization line and melting lines cross each other at finite values of d_c^{-1}.

Experiments on other systems (i-polypropylene, i-polystyrene, polyethylene, poly(1-butene), poly(ϵ-caprolactone)) showed the same general scenario[2].

The observations demonstrated that different laws control crystallization and melting, or, in other words, that crystallization and melting are not reverse processes. The validity of the Gibbs-Thomson equation and the observed depression of melting temperatures if co-units are present in the melt indicate that the melting process is based on a direct transfer of chain sequences from lateral crystal surfaces into the contacting melt. Crystal formation follows another pathway. This is shown by the independence of crystal thicknesses on the tacticity or the co-unit content and the control of the thickness value by

a temperature, which is different from the equilibrium melting point. We interpret the observations as indication that the pathway followed in the formation of crystals includes an intermediate phase of mesomorphic character. Some years ago, we proposed as a first qualitative picture a certain multistage route[3]. A thin layer with mesomorphic inner structure forms between the lateral crystal surface and the melt, stabilized by epitaxial forces. The first step in the growth process is an attachment of chain sequences from the melt onto the growth face of the mesomorphic layer. The high mobility of the chains in the layer allows a spontaneous thickening, up to a critical thickness, where the layer solidifies under formation of block-like crystallites. The last step is a perfectioning of the crystallites, leading to a further stabilization.

For the crystallization temperatures chosen in the experiments of Fig. 1 all crystallites kept their thickness constant up to the melting point. A different behavior is observed when the crystallization is carried out at lower temperatures, down to temperatures near T_{g}. When heating such a sample after the completion of the crystallization, reorganization processes set in. They continue up to the final melting at some characteristic temperature which is independent of the initially chosen crystallization temperature. We report in this work the results of corresponding SAXS measurements, again carried out for different s-polypropylenes. The results show that recrystallization processes obey over an extended temperature range a simple law which commonly holds for all samples, independent of their tacticity or the co-unit content. DSC thermograms show a multi-peak structure. The SAXS data allow an interpretation and an assignment of the peaks.

2 Experimental Details

2.1 Materials

Experiments were carried out for three samples which cover a large range of melting points and crystallinities:

- The first sample, named 'sPP', was synthesized in the Institute of Macromolecular Chemistry of our university in the group of Rolf Mülhaupt. With only 3% of mesodiades it has the highest tacticity. Crystallinities at the end of isothermal crystallization processes are in the range $\phi_c \approx 0.3$; temperatures of final melting vary between $140^\circ\mathrm{C}$ and $160^\circ\mathrm{C}$ in dependence on T_c.

- The second sample, named 'sPP-Mitsui', is a commercial product. The crystallinity is $\phi_c \approx 0.2$, and the temperatures of final melting are in the range of $120^\circ\mathrm{C}$ to $140^\circ\mathrm{C}$.

- The third sample is a random copolymer with 20 weight percent of octene units, named 'sP(PcO20)'. It was also synthesized in Mülhaupt's group. Its crystallinity is about 10%; melting occurs in the range of $80^\circ\mathrm{C}$ to $100^\circ\mathrm{C}$.

2.2 Instrumentation

SAXS experiments were carried out with the aid of a Kratky camera attached to a conventional Cu K_α X-ray source using a temperature controlled sample holder. Employing a position sensitive metal wire detector, scattering curves were usually registered within 5 to 10 minutes counting time. An algorithm developed in our group was applied in the deconvolution of the slit-smeared scattering data. In order to remove all memory effects, samples were kept in the melt at $200^\circ\mathrm{C}$ for about 10 minutes before starting an experiment. The cooling to the chosen crystallization temperature was carried out as quickly as possible, typically within 2-3 minutes. By observation of the intensity it was ensured that crystallization did not start before reaching isothermal conditions.

For the registration of DSC thermograms we used a Perkin Elmer DSC 4. Weight fraction crystallinities were derived from the heat of fusion, by taking the ratio to the ideal value ΔH_{id} of a fully crystalline sample. We assumed as in previous works $\Delta H_{\mathrm{id}} = 183\ \mathrm{Jg}^{-1}$.

2.3 SAXS Data Analysis

Having determined the primary beam intensity with the aid of a moving slit system, desmeared scattering curves were obtained in absolute values, as differential cross sections per unit volume, $\Sigma(q)$. With a knowledge of $\Sigma(q)$ the one-dimensional electron density auto correlation function $K(z)$ and its second derivative $K''(z)$, which gives the interface distance distribution function (IDF) [4], were calculated applying the Fourier relations

$$K(z) = \frac{1}{r_{\mathrm{e}}^2}\frac{1}{(2\pi)^3}\int_0^\infty \cos qz \cdot 4\pi q^2 \Sigma(q)\mathrm{d}q \tag{1}$$

and

$$K''(z) = \frac{2}{r_{\mathrm{e}}^2(2\pi)^2}\int_0^\infty [\lim_{q\to\infty} q^4\Sigma(q) - q^4\Sigma(q)]\cos qz\mathrm{d}q \ . \tag{2}$$

Here, q denotes the scattering vector $q = 4\pi \sin\theta_B/\lambda$ (θ_B: Bragg scattering angle); r_{e} is the classical electron radius.

In all the measurements the crystal thickness d_{c} was derived from the location of the respective peak in $K''(z)$. d_{c} represents a well-defined quantity, opposite to the varying thickness of the amorphous intercrystalline regions. Correspondingly only one peak is generally found in the IDF, and its location gives d_{c}.

A useful parameter in the analysis of the continuous melting on heating is the Porod coefficient P. It generally determines for two-phase systems the asymptotic behavior of the scattering curve as

$$\lim_{q\to\infty}\Sigma(q) = r_{\mathrm{e}}^2\frac{P}{(q/2\pi)^4} \ . \tag{3}$$

The Porod coefficient is directly related to the interface area per unit volume O_{ac}, by

$$P = \frac{1}{8\pi^3}O_{\mathrm{ac}}(\rho_{\mathrm{e,c}} - \rho_{\mathrm{e,a}})^2 \ , \tag{4}$$

where $\rho_{\mathrm{e,c}}$ and $\rho_{\mathrm{e,a}}$ denote the electron densities of the crystals and the melt respectively. This relation

is generally valid, for homogeneous as well as for heterogeneous structures and therefore, for example, also in the main melting region.

Prerequisite of a data evaluation based on $K(z)$ or $K"(z)$ is the existence of layer-like crystallites in the sample which are flat over distances larger than the crystal thickness. While this is ensured for a crystallization at high temperature, it should be checked, when the crystallization process is conducted at larger supercoolings. We did this for the sample with the lowest crystallinity, sP(PcO20), using an atomic force microscope (AFM). Fig. 2 presents a tapping mode image obtained after a crystallization at $20^{\circ}\mathrm{C}$. To see the bulk properties, the sample was cut at cryogenic temperatures and then scanned at room temperature. The dominant feature are layer-like crystallites. There are no stacks built up of many layers, as is usually found at low supercoolings, but this is not required for the one-dimensional correlation function analysis.

3 Results

Figs. 3, 4, 5 present DSC thermograms obtained for the three samples under study. Measurements always started at the crystallization temperature after completion of the crystallization process. Each figure contains a series of thermograms measured for a series of T_{c}s.

For sPP (Fig. 3) two types of thermograms were obtained in dependence on the crystallization temperature:

- For $T_{\mathrm{c}} \geq 115^{\circ}\mathrm{C}$ one melting peak is observed, which shifts to higher temperatures with increasing T_{c}.

- For all lower temperatures, i.e., $T_{\mathrm{c}} < 115^{\circ}\mathrm{C}$, the thermogram has two peaks. The one at higher temperature associated with the final melting is constantly located at $145^{\circ}\mathrm{C}$. The second peak shifts to lower temperatures with falling T_{c} and simultaneously decreases in height.

The same general properties show up in the series of thermograms obtained for sPP-Mitsui (Fig. 4). Here,

the critical crystallization temperature is at 105°C . One peak is found from this temperature upwards, and two peaks for lower temperatures, with a final melting always at 135°C . All these thermograms were measured with a heating rate of 10K/min.

Characteristic changes with T_c are also observed for sP(PcO20). Fig. 5 shows thermograms measured after crystallizations at 20°C , 40°C , 60°C and 80°C , now not only for a heating rate of 10K/min, but also for 3K/min and 1K/min. For T_c=20°C and 40°C three peaks are found, named A, I and R. Their locations and amplitudes vary with T_c and the heating rate, but in different manner. Peak R relates to the final melting which is completed at 95°C . It therefore corresponds to the high temperature endotherm at constant position in Figs. 3 and 4 for sPP and sPP-Mitsui when crystallized below 115°C and 105°C , respectively. Peak I varies with T_c in the same manner as the low temperature endotherms of sPP and sPP-Mitsui in Figs. 3 and 4. The new feature in the thermograms of sP(PcO20) is the third peak, denoted A. It shifts to higher temperatures and increases its amplitude when the heating rate is raised. In fact, a low temperature endotherm with the properties of peak A has already been observed in many crystallizing polymers, and is commonly addressed as 'annealing peak'. A recent work of the Schick group on poly(ethylene terephthalate) using high speed calorimetry reveals that this peak is the result of a melting-recrystallization process involving a large part of the crystallites in the sample, rather than representing the melting of only a few crystallites with low stability, as was assumed earlier [5]. The changes with the heating rate in the thermograms corroborate this view. At higher T_cs thermograms become simpler in structure. Peak R has disappeared for T_c=60°C , and for T_c=80°C only peak I is left. The critical temperature of sp(PcO20) is around 60°C . Below this crystallization temperature melting is always completed at about 95°C - the location of the maximum of the broad peak associated with the final melting is at 85°C -90°C . For T_cs from 60°C upwards melting points are above 90°C and vary together with T_c.

Heating rate effects exist also for sPP and sPP-Mitsui. Fig. 6 shows this for sPP crystallized at 80°C . Reducing the heating rate results in a drop of the amplitude of the first peak (I) and a corresponding

increase of the second peak (R) at the final melting temperature. The lowest heating rate chosen, 1K/min, is not too far away from the mean heating rate of about 0.2K/min associated with the stepwise temperature rises in the SAXS measurements. According to the thermograms, at such a heating rate the first peak (I) practically vanishes.

The results of all SAXS experiments are collected in Fig. 7. Samples were isothermally crystallized and then heated in steps of 3K. The SAXS patterns, registered with a position-sensitive detector, were evaluated and the crystal thicknesses determined as described in Section 2.3. The figures present the variation of the thickness during a heating up to the melting point, in plots of d_c^{-1} versus the temperature. The inverse initial thickness - determined after completion of the isothermal crystallization process - is shown for all samples and T_cs by a filled square. Corroborating the previous results, all these points are located on the crystallization line shown in Fig. 1 which is again included in the diagrams. The curves starting off from the initial points depict the values of d_c^{-1} determined during the stepwise heating. After each temperature step a new stationary state was rapidly established; checks did not show any later changes. In agreement with the DSC results two different behaviors are found during heating in dependence on T_c:

- For sufficiently high T_cs the crystal thickness remains constant up to the melting point. SAXS based melting points, identified with the temperature at which the Porod coefficient shows the largest drop, and DSC melting points agree with each other.

- For T_cs in the low temperature region heating is accompanied by a continuous crystal thickening indicative for overall reorganization processes. Recrystallization goes on up to the temperature of final melting, indicated by a star. As is shown for sPP and sP(PcO20), this temperature of final melting does not change with T_c.

Of particular interest are the details of the thickening process. In the case of sP(PcO) crystallized at $20^\circ\mathrm{C}$ heating leaves the crystal thickness at first constant. This changes at $50^\circ\mathrm{C}$. Here thickening processes set in, and the further course is well defined: d_c^{-1} changes linearly with temperature following

the drawn straight line. Recrystallization ends at 85°C with the melting. The same linear dependence shows up when sP(PcO20) is at first crystallized at 40°C . Recrystallization again sets in when the line is reached, and d_c^{-1} follows this line from thereon, up to the final melting at 85°C . Fig. 8 shows the related changes in the Porod coefficient. When the d_c values agree, the Porod coefficients become also identical. Obviously, from thereon one has equal structures. For all T_cs both samples are completely molten at 95°C , in agreement with the DSC results.

The line in the diagram guiding the process of recrystallization for sP(PcO20) controls also the recrystallization for the other two samples. The line is equally included in all three figures in Fig. 7. As can be seen, recrystallization of sPP and sPP-Mitsui leads over an extended temperature range to the same linear dependence of d_c^{-1} on T as for sP(PcO20). This begins when during heating the guiding line is reached for the first time. Different between sPP, sPP-Mitsui and sP(PcO20) is the behavior at the beginning of heating. For the first two samples, reorganization processes set in immediately, whereas the d_c values of sP(PcO20) remain constant over the first 30 degrees. The 'recrystallization line' which controls in this manner the recrystallization processes commonly for all samples has a characteristic property: Extrapolation of the line to $d_c^{-1} \to 0$ ends at the same temperature as the crystallization line, namely at T_c^{∞} =195°C .

Fig. 9 shows another property of the recrystallization process, here for sPP: The linear crystallinity $\phi_{\rm lin} = d_c/L$ remains constant up to the range of final melting. This holds in spite of the large changes in d_c and the long spacing L, and in spite of the continuous melting showing up in $P(T)$.

4 Discussion

The described results suggest the validity of a simple scheme for the description of crystallization, recrystallization and melting processes which can be commonly applied to all sorts of sPPs and related statistical copolymers. The scheme can be established using a d_c^{-1}/T-diagram and is presented in Fig. 10. The diagram is composed of three lines,

- the crystallization line representing the relationship between the crystallization temperature $T_{\rm c}$ and the inverse crystal thickness $d_{\rm c}^{-1}$, as being given by

$$d_{\rm c}^{-1} = C_{\rm c}(T_{\rm c}^{\infty} - T_{\rm c}) \qquad (T_{\rm c}^{\infty} = 195^{\circ}{\rm C}\ )\ , \tag{5}$$

- the recrystallization line controlling the course of recrystallization processes being given by

$$d_{\rm c}^{-1} = C_{\rm r}(T_{\rm c}^{\infty} - T) \tag{6}$$

  with $C_{\rm r} < C_{\rm c}$,

- the melting line with all final melting points $T_{\rm f}$, being given by the Gibbs-Thomson equation

$$d_{\rm c}^{-1} = C_{\rm m}(T_{\rm f}^{\infty} - T_{\rm f}) \tag{7}$$

  (plotted for sPP-Mitsui with $T_{\rm f}^{\infty}$ = 162°C).

Crystallization line and recrystallization line are sample-invariant, i.e., they are not affected by the tacticity or the co-unit content. The melting line, on the other hand, shifts to lower temperatures when the chemical disorder in the chain increases. Melting line and recrystallization line intersect each other at a certain temperature and a certain value of $d_{\rm c}^{-1}$. This point of intersection, denoted $X_{\rm s}$ in Fig. 10, marks the end of recrystallization processes. If the initial value of the crystal thickness is above the thickness value at $X_{\rm s}$ no recrystallization occurs; the sample just melts. For an initial thickness below the critical value one has always recrystallization before melting. Whenever the recrystallization line is reached during a heating experiment, $d_{\rm c}^{-1}$ varies linearly with T guided by the line, up to the temperature at $X_{\rm s}$ where the crystals melt. This temperature of final melting varies between different samples according to the displacement of $X_{\rm s}$.

Non-predictable on the basis of the present findings is only the passage from the crystallization line at the beginning to the recrystallization line. A simple behavior is found for P(PcO20), where $d_{\rm c}^{-1}$ remains constant until the recrystallization line is reached. The crystals of the two other samples behave

differently. Reorganization processes begin immediately above T_c, and the crystallites have already thickened when the recrystallization line is reached.

Which is the physical background of the endotherm 'I' which appears for lower T_cs for all samples prior to the final melting? Fig. 11 gives the answer for sPP: All these peaks - observed for crystallization temperatures below $80^\circ\mathrm{C}$ and $100^\circ\mathrm{C}$ - have a location on the melting line, then when the construction introduced in the figure is applied. The construction assumes absence of any thickness changes during the heating. Then the melting point lies on the vertical line starting off from the initial state. Placing the temperatures of peak I on the vertical lines going up from the crystallization line for the different T_cs yields the set of crossed spheres. It is seen that they are all exactly located on the melting line. The result means that part of the crystallites is not included in the reorganization process and melts directly without any thickening. Fig. 6 demonstrates that this fraction depends on the heating rate; it is lowered when the heating rate decreases. For the heating rates realized in the SAXS experiments, the peak practically vanishes. As it appears, under these conditions recrystallization involves all crystallites in the sample.

Analogous results are obtained for sPP-Mitsui and for the endotherms I in the thermograms of sP(PcO20). The positions of the latter ones are shown in Fig.12 applying the same construction as in Fig.11. As to be noted, the peaks 'I' are also placed on the melting line.

The results for sPP displayed in Fig. 9 show that recrystallization can result in continuous changes in the length scales of the structure as given by d_c and L under conditions of a constant linear crystallinity, and up to about $90^\circ\mathrm{C}$ also a constant global crystallinity. This means that recrystallization is an overall process which affects all crystallites equally so that homogeneity is retained. Whether or not homogeneity is preserved depends, however, on the time provided, i.e. the heating rate, and this in different manner for the three samples. As the thermogram for sP(PcO20) shows, for a heating rate of 10K/min the structural reorganization is no longer uniform. Part of the crystallites melts already in the range of the annealing peak, a second fraction does not participate in the recrystallization and melts with the endotherm I, and only a minor fraction of material takes part in the recrystallization process. For the

very low effective heating rates realized in the SAXS experiments again a large part of the structure takes part in the reformation process, but the drop of the global crystallinity sets in earlier as is indicated by the Porod coefficient.

Which conclusions can be drawn from the validity of the scheme - and we think it holds generally, not only for s-polypropylene? It was already clear that formation and melting of polymer crystals are not reverse processes. Now it is seen in addition that crystallization and recrystallization are intimately related. Both are

- independent of the co-unit content and the tacticity of chains
- controlled by the supercooling below the same temperature, T_c^∞, which is located above the equilibrium melting point.

We understand these findings as indicating that not only the crystallization but also the recrystallization processes pass over a transient mesophase. Recrystallization is a very fast process, much faster then the first crystallization out of a relaxed melt. It is therefore conceivable to envisage it as being mediated by short transitions into a mesomorphic rather than the molten state. All the crystal blocks could commonly soften in this way thus enabling a cooperative reorganization of whole stacks. When blocks with a larger size have formed, a new solidification takes place.

Even if these processes are in general very rapid, they are apparently not fast enough under all conditions everywhere in the sample. For temperatures just below the intersection point X_s one observes on time scales corresponding to standard DSC heating rates always also a melting of non-recrystallized parts. Melting proceeds by a detachment of chain sequences from lateral crystal faces into the adjacent melts. If block softening and thickening is retarded a direct melting from the crystal surfaces apparently gains the priority.

The finding of a sample invariant course of the recrystallization processes is new, but the scheme of Fig. 10 has already been proposed a year ago [6]. When the scheme was introduced, thermodynamic assignments were given to all lines. They are all interpreted as loci of size dependent phase transitions,

dealing with four different phases:

- the amorphous melt
- mesomorphic layers

and, in order to account for the stabilization processes, two limiting forms of the crystallites, namely

- native crystals and
- stabilized crystals .

The crystallization line is associated with a transition of a mesomorphic layer into a native crystalline form, the recrystallization line is the locus of transitions between mesomorphic and stabilized crystal blocks, and the melting line describes the melting points of stabilized crystallites. The scheme implies the existence of a sample invariant recrystallization line, but this invariance was not demonstrated at the time of its introduction. The experiments reported here show that it is indeed found and thus corroborate our views.

Acknowledgements

Support of this work by the Deutsche Forschungsgemeinschaft (Sonderforschungsbereich 428) is gratefully acknowledged. Thanks are also due to the Fonds der Chemischen Industrie for financial help.

References

[1] G. Hauser, J. Schmidtke, and G. Strobl. *Macromolecules*, 31:6250, 1998.

[2] G. Strobl. *Progr. Polym. Sci.*, 31:398, 2006.

[3] G. Strobl. *Eur.Phys.J.E*, 3:165, 2000.

[4] W. Ruland. *Colloid Polym.Sci.*, 255:417, 1977.

[5] A.A. Minakov, D.A. Mordvintsev, and C. Schick. *Polymer*, 45:3755, 2004.

[6] G. Strobl. *Eur.Phys.J.E*, 18:295, 2005.

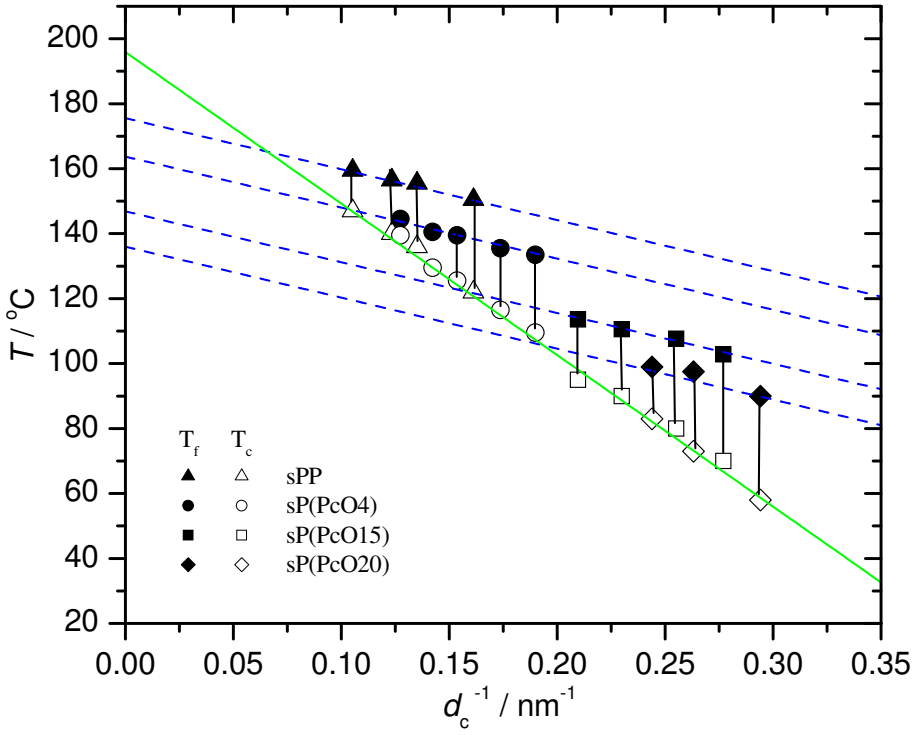

Figure 1: s-polypropylene (sPP) and s-propene octene copolymers (sP(PcOx), x:% per weight) : Unique crystallization line (*open symbols*) and series of melting lines (*filled symbols*). From [1]

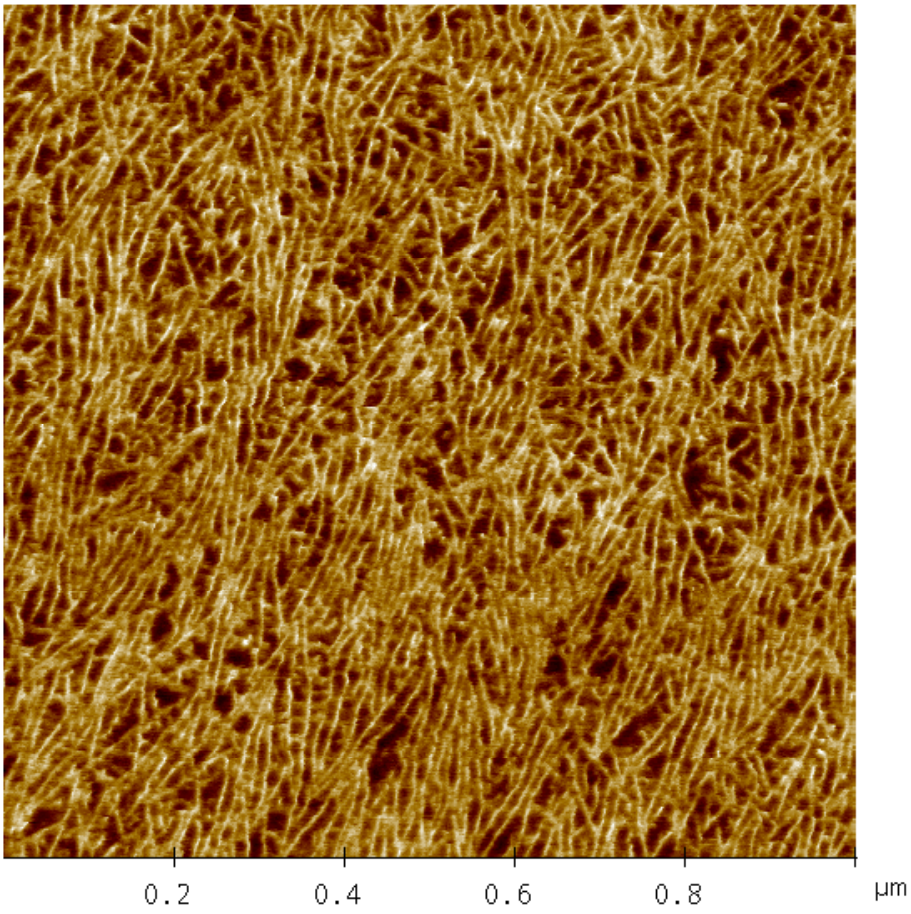

Figure 2: sP(PcO20), crystallized at 20°C : AFM tapping mode image of a surface created by cutting a sample at cryogenic temperatures

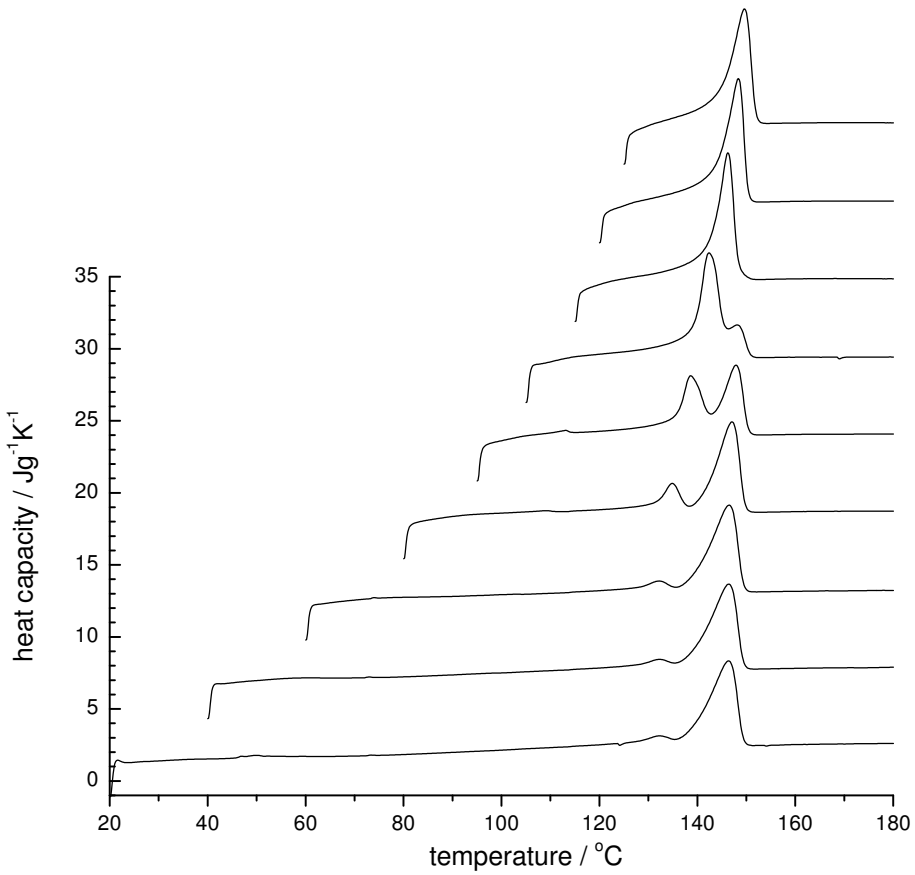

Figure 3: sPP, crystallized at various temperatures followed by a heating to the melt: DSC curves obtained with a heating rate of 10K/min

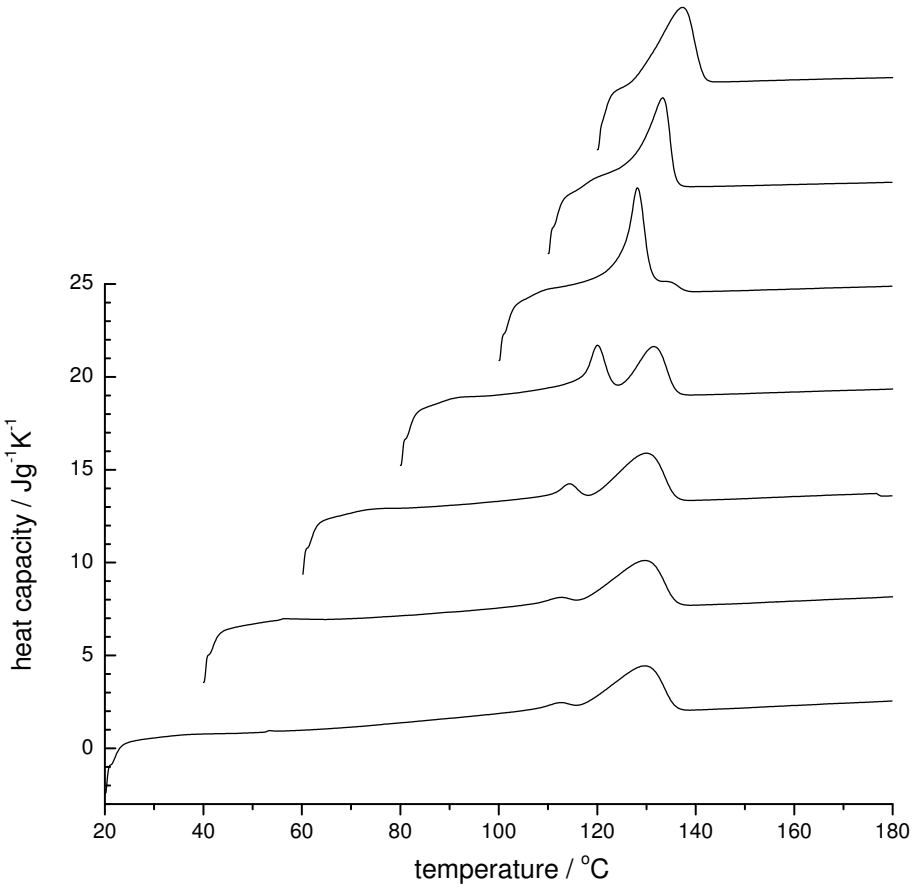

Figure 4: sPP-Mitsui, crystallized at various temperatures followed by a heating to the melt: DSC curves obtained with a heating rate of 10K/min

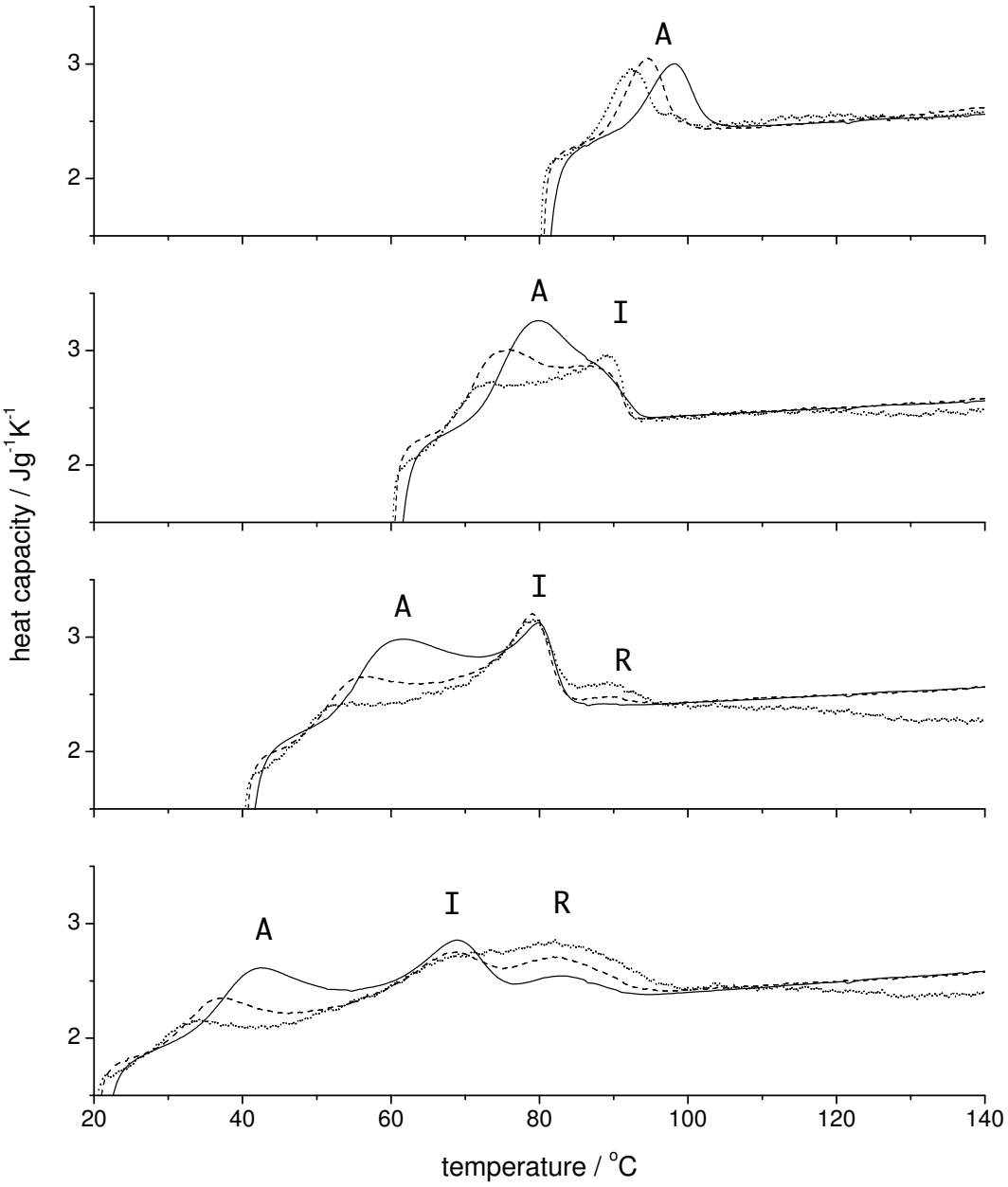

Figure 5: sP(PcO20), crystallized at 20°C (*bottom*), 40°C , 60°C and 80°C (*top*) followed by a heating to the melt: DSC curves obtained with heating rates of 10K/min , 3K/min (*dashed*) and 1K/min (*dotted*)

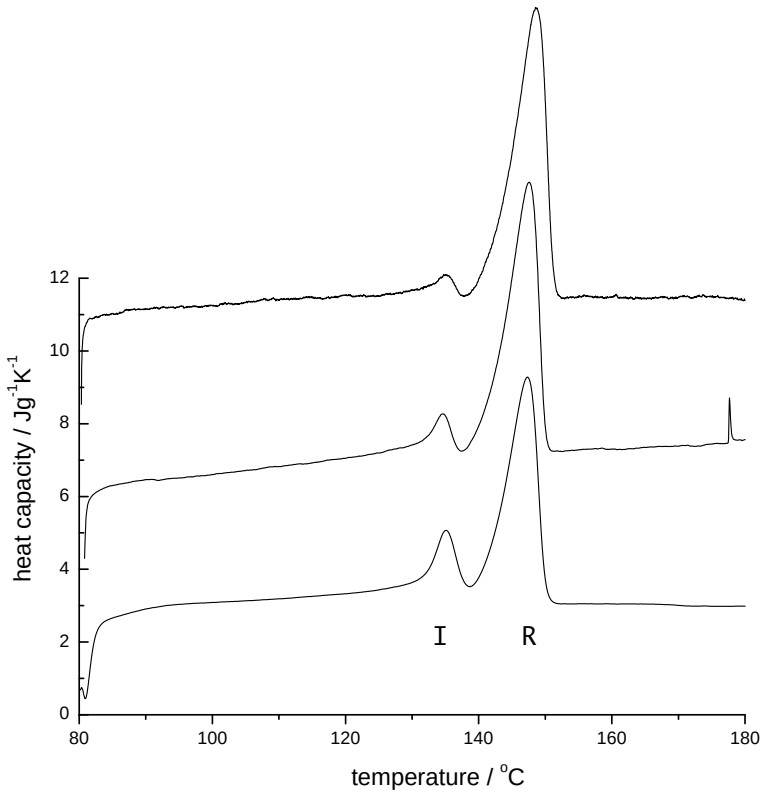

Figure 6: sPP, crystallized at 80°C followed by a heating to the melt: DSC curves obtained with heating rates of 10K/min (*bottom*), 3K/min and 1K/min (*top*)

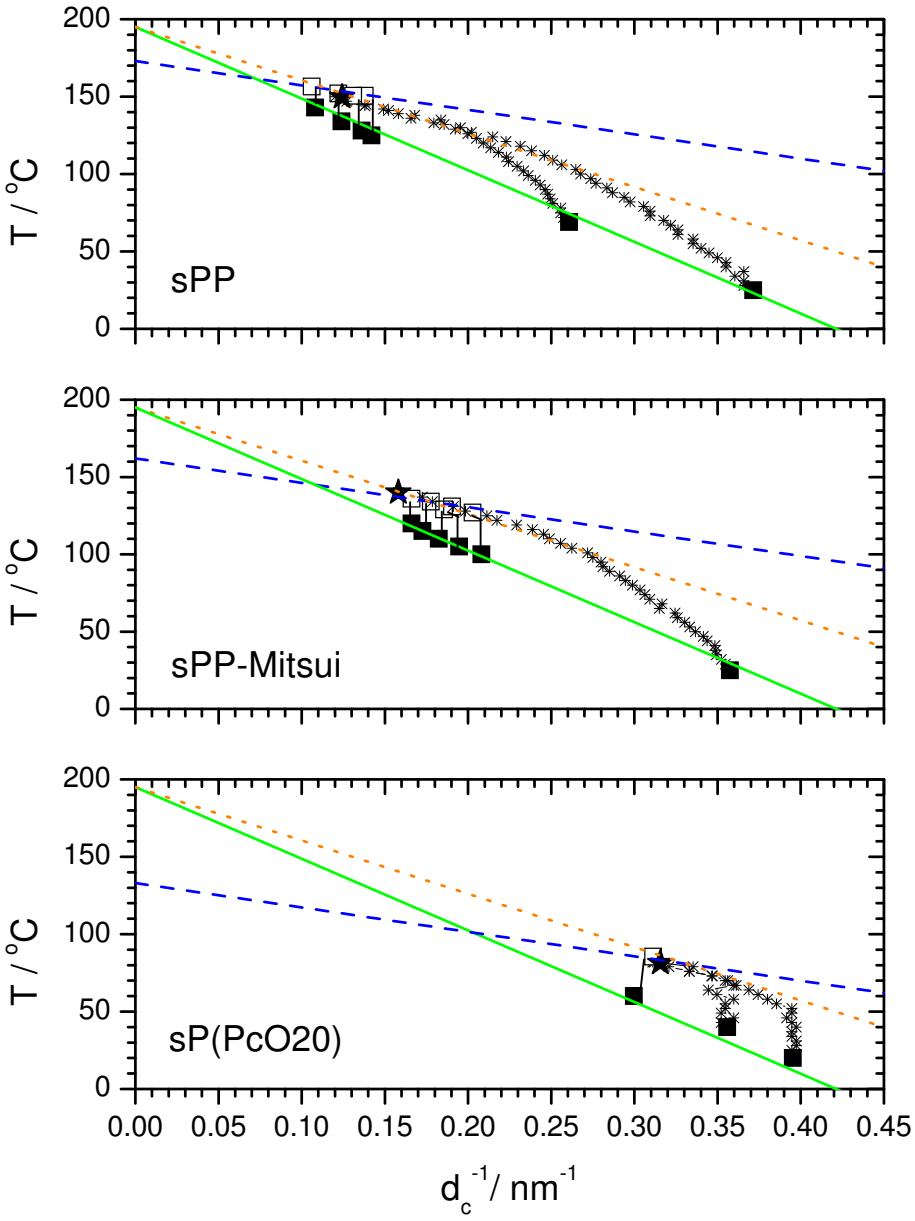

Figure 7: sPP, sPP-Mitsui, sP(PcO20), crystallized at various T_cs and heated: Inverse crystal thicknesses at T_c (*filled squares*), at melting points (*open squares*) and at the ending of recrystallization (*stars*). All crystallization lines and recrystallization lines (*dots*) are identical, the melting lines (*dashes*) have a common slope but are shifted against each other

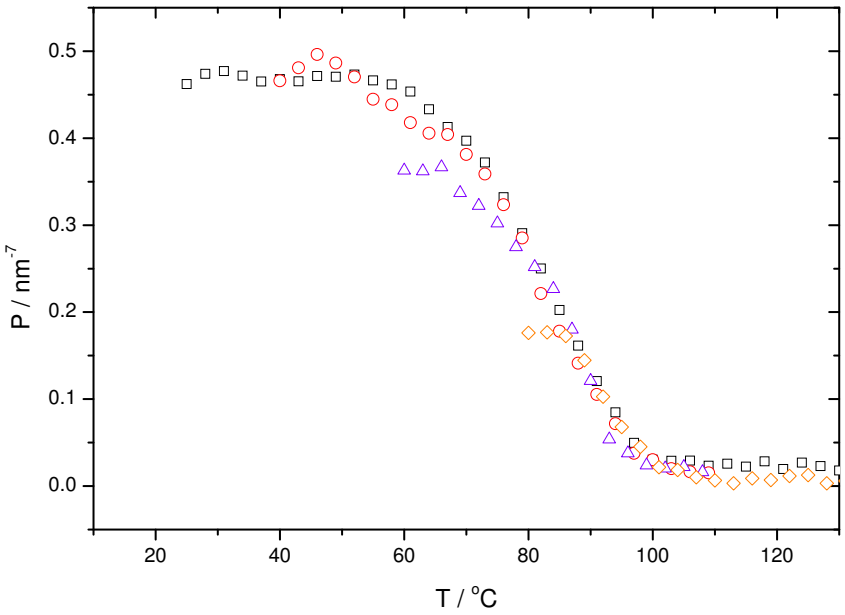

Figure 8: sP(PcO20), crystallized at 20°C (*squares*), 40°C (*circles*) and 60°C (*triangles*): Variation of the Porod coefficient during heating

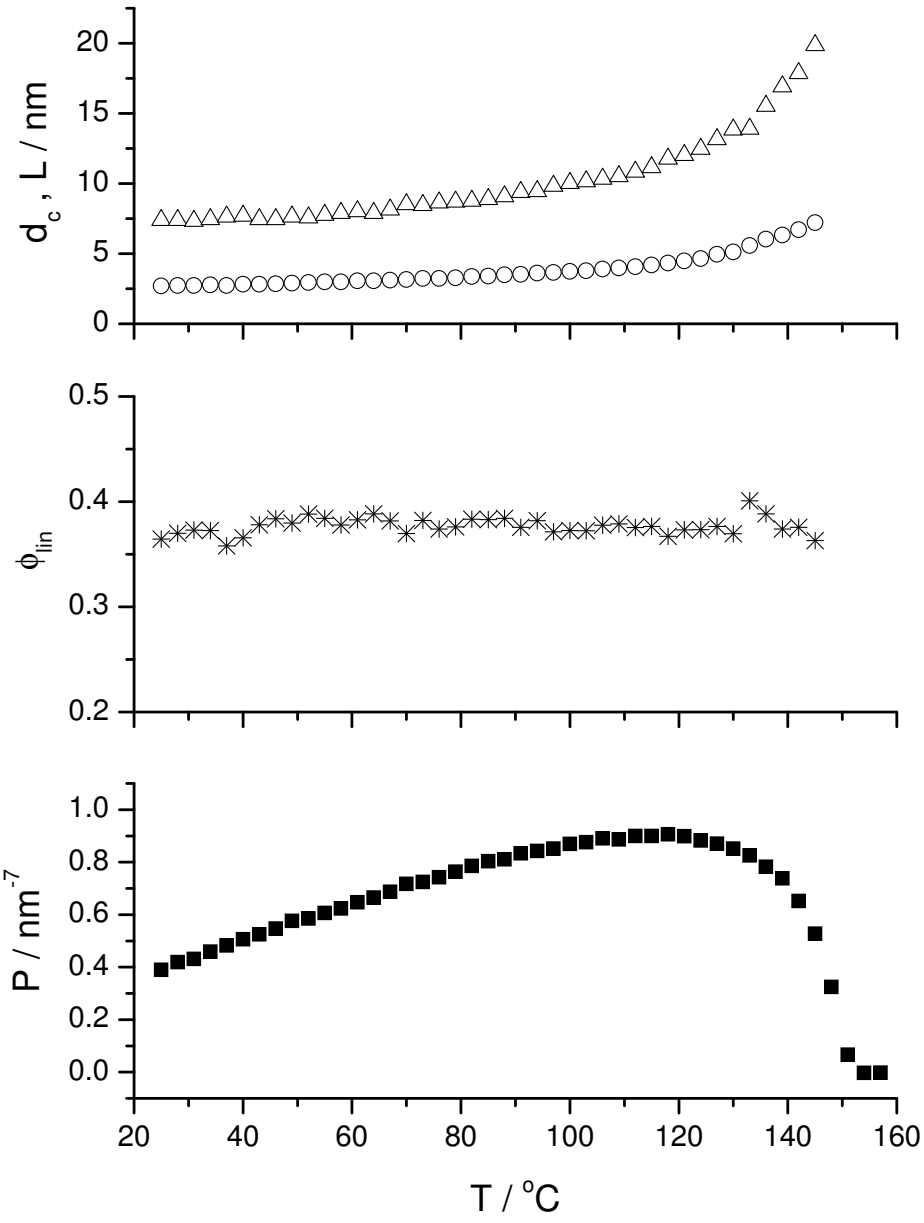

Figure 9: sPP, crystallized at 25°C and heated up to the melt: Temperature dependencies of (*top*) crystal thickness and long spacing L, (*center*) the linear crystallinity $\phi_{\mathrm{lin}} = d_{\mathrm{c}}/L$, and (*bottom*) the Porod coefficient

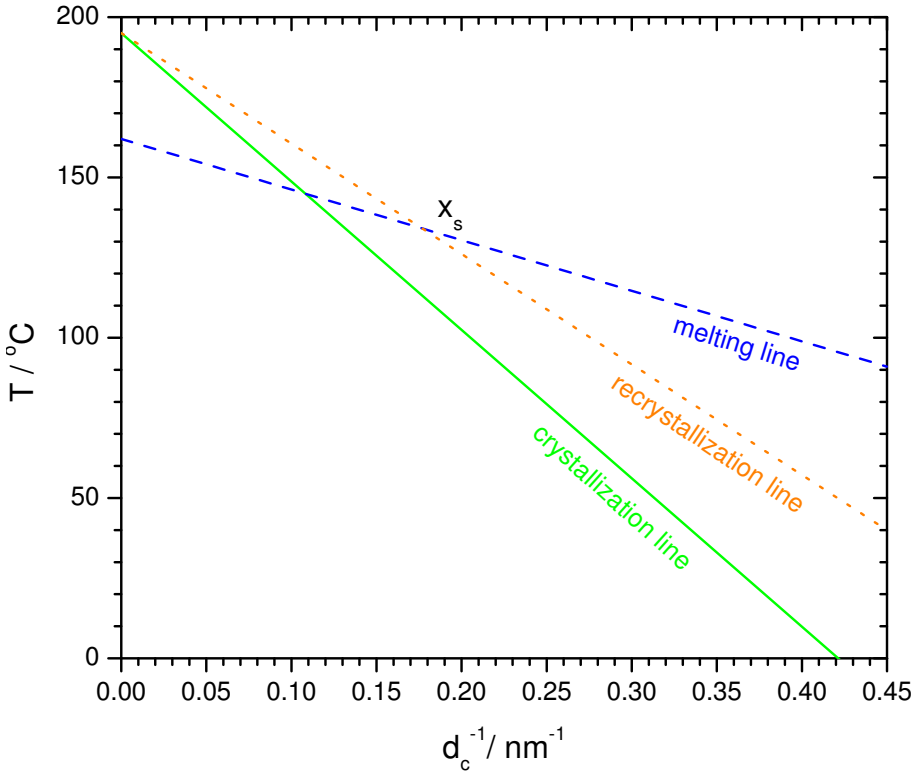

Figure 10: A general scheme treating crystallization, recrystallization and melting of s-polypropylene : Common crystallization line, common recrystallization line, sample dependent melting line (here: for sPP-Mitsui)

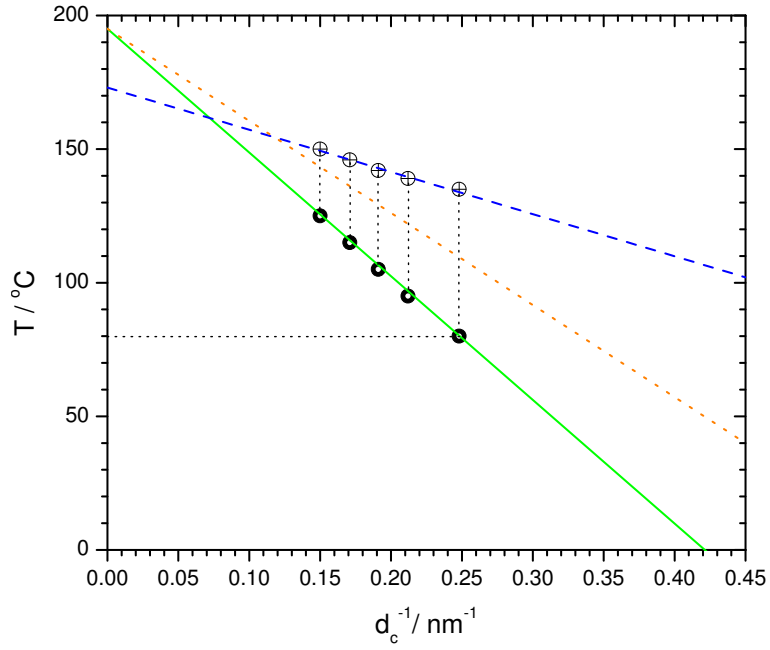

Figure 11: sPP, crystallization line, recrystallization line and melting line as in Fig. 7. Melting points of the initial crystallites as given by the peaks '*I*'in the DSC thermograms: They are indeed located on the melting line

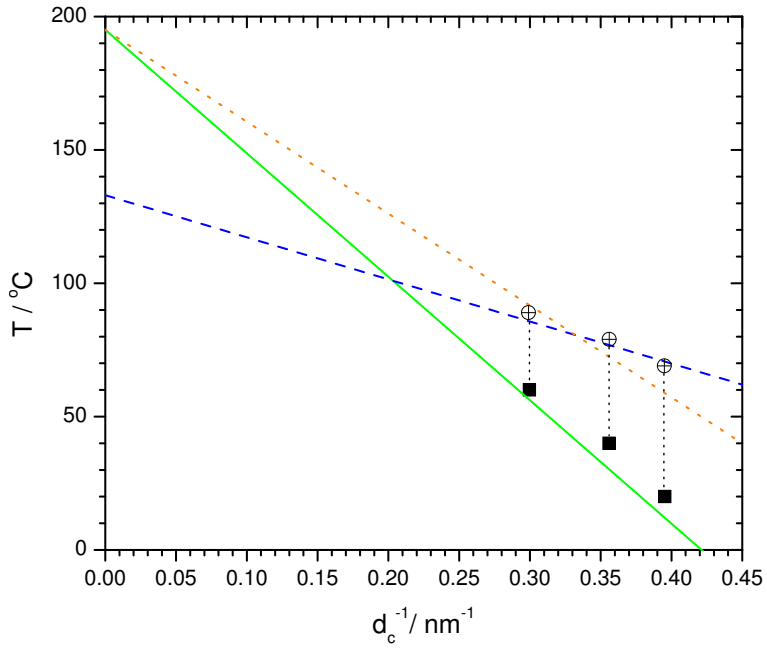

Figure 12: sP(PcO20), crystallization line, recrystallization line and melting line from Fig. 7. Locations of the I-peaks in the DSC curves